



POLİTEKNİK DERGİSİ

JOURNAL of POLYTECHNIC

ISSN: 1302-0900 (PRINT), ISSN: 2147-9429 (ONLINE)

URL: <http://dergipark.org.tr/politeknik>



Determination of non-ionizing radiation and shielding studies of a new dc plasma device

Yeni bir dc plazma cihazında iyonize olmayan radyasyonun belirlenmesi ve ekranlama çalışmaları

Yazar(lar) (Author(s)): Nihan Merve SARIKAHYA¹, Mehmet SARIKAHYA², Erol KURT³

*ORCID*¹: 0009-0003-8143-9743

*ORCID*²: 0000-0002-0966-2057

*ORCID*³: 0000-0002-3615-6926

To cite to this article: Sarıkahya N. M., Sarıkahya M. ve Kurt E., “Determination of non-ionizing radiation and shielding studies of a new dc plasma device”, *Journal of Polytechnic*, 27(1): 397-406, (2024).

Bu makaleye şu şekilde atıfta bulunabilirsiniz: Sarıkahya N. M., Sarıkahya M. ve Kurt E., “Determination of non-ionizing radiation and shielding studies of a new dc plasma device”, *Politeknik Dergisi*, 27(1): 397-406, (2024).

Erişim linki (To link to this article): <http://dergipark.org.tr/politeknik/archive>

DOI: 10.2339/politeknik.1281625

Determination of Non-ionizing Radiation and Shielding Studies of a New DC Plasma Device

Highlights

- ❖ DC plasma
- ❖ Electromagnetic shielding
- ❖ Electromagnetic interference (EMI)
- ❖ Non-ionizing radiation
- ❖ Shielding Effectiveness

Graphical Abstract

Figure 1 summarizes the SE value at three directions for three shielding materials which are honeycomb, swatter and square. The highest shielding value is provided by the swatter at different directions. A shielding value of over 20 dB is only provided for the swatter.

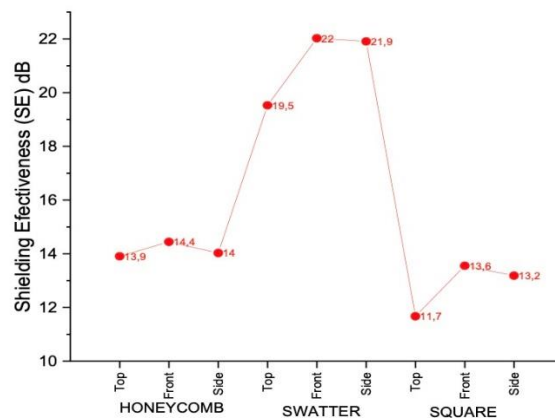


Figure. The shielding effectiveness of the plasma device for different shielding methods

Aim

The aim is the determination of the electromagnetic radiation and shielding studies of a new designed and constructed portative plasma device

Design & Methodology

The device works with high voltage up to 2 kV depending on its filling gas pressure and contains a couple of terminals in the low pressurized chamber. As the methodology, different shielding materials with different geometries are applied.

Originality

Swatter, honeycomb and square models's shielding effectiveness are compared..

Findings

The best shielding effectiveness for the new plasma device from all of the directions is provided by the swatter cage material since it gives the best fit for the wavelength of the generated radiation.

Conclusion

It is observed that the shape of the shielding material is very important for the optimum shielding.

Declaration of Ethical Standards

The author(s) of this article declare that the materials and methods used in this study do not require ethical committee permission and/or legal-special permission

Yeni Bir DC Plazma Cihazında İyonize Olmayan Radyasyonun Belirlenmesi ve Ekranlama Çalışmaları

Araştırma Makalesi / Research Article

Nihan Merve SARIKAHYA*, Mehmet SARIKAHYA, Erol KURT

Teknoloji Fakültesi, Elektrik Elektronik Mühendisliği Bölümü, Gazi Üniversitesi, Türkiye

(Geliş/Received : 12.04.2023 ; Kabul/Accepted : 25.05.2023 ; Erken Görünüm/Early View : 11.09.2023)

ÖZ

Bu çalışmada, yeni tasarlanan ve üretilen portatif plazma cihazının elektromanyetik alan ölçümleri ve ekranlama çalışmaları yapılmıştır. Cihaz, dolun gazı basıncına bağlı olarak 2 kV'a kadar yüksek voltajla çalışmaktadır ve düşük basınçlı haznede elektrik ve manyetik alanları hapsedilmiş plazma yapıları oluşturmak için bir çift terminal içermektedir. Basit bir torus geometrisi olan hazne, plazma kararlılığı araştırmaları için He gazı ile çalıştırılmaktadır. Cihazdan farklı mesafelerde elektromanyetik alan değerleri ölçümü yapılmış ve iyonlaştırıcı olmayan radyasyonu önlemek için farklı ekranlama malzemeleri (Swatter, Square, Honeycomb) kullanılmıştır. Farklı malzemelerle yapılan ölçüm sonuçlarına göre, optimum ekranlama değeri elde etmek için ekranlama malzemesinin şeklinin çok önemli olduğu görülmüştür.

Anahtar Kelimeler: DC plazma, ekranlama, elektromanyetik girişim (EMG), iyonlaştırıcı olmayan radyasyon.

Determination of Non-ionizing Radiation and Shielding Studies of a New DC Plasma Device

ABSTRACT

In the present work, the determination of the electromagnetic radiation and shielding studies of a new designed and constructed portative plasma device have been reported. For this aim, the electromagnetic interference (EMI) measurements are performed. The device works with high voltage up to 2 kV depending on its filling gas pressure and contains a couple of terminals in the low pressurized chamber to form plasma structures confined in terms of electrical and magnetic confinement. The chamber as a simple torus geometry has been operated with He gas for the plasma stability explorations. The EMI measurements have been practiced for different distances from the setup and used different shielding materials to prevent the non-ionizing radiation. According to detailed tests with different shielding materials (Swatter, Square, Honeycomb) it is observed that the shape of the shielding material is very important for the optimum shielding results.

Keywords: DC plasma, shielding, electromagnetic interference (EMI), non-ionizing radiation.

1. INTRODUCTION

The electromagnetic confinement techniques are vital for forming a stable plasma media. As the main energy source of future generations, fusion energy gets more and more interest from the scientific world [1,2]. Strictly speaking, plasma studies can be classified as cold and hot plasma studies. Among them, cold plasma is used widely for etching of materials, ion feeding and other material processing tasks including the semiconductors, conductors, superconductors and dielectrics. In addition, cold plasmas are encountered in many medicine, defense industry, aviation industry systems. On the other hand, hot plasmas are mostly required for fusion technology, where energy release occurs by combining two or more atomic nuclei in accordance with Einstein's theory. For this, especially Deuterium and Tritium nuclei are tested world-widely. In any DC plasma device, ions are

continuously accelerated by a constant negative potential between the electrodes, where negative charges (i.e. electrons) are accelerated towards positive electrode.

Apart from the pulsed plasma devices where fusion events occur for specific gases like Deuterium and Tritium on the nanosecond scale, dc plasma devices require durable electrode materials made from Wolfram [1]. Either the plasma device operates in pulsed or continuous mode, the main concern is providing the stability of the plasma formation since the surface of electrodes and the non-equilibrium plasma media change by time after applying the high voltage from external sources. Indeed, many of the devices operate at the order of several kV scale and fed by a DC current, therefore they should be stabilized electrically in order to perform a good plasma media during the entire operation.

According to the literature, the power source makes possible the confinement of the Deuterium ions under a kV-scaled electrical potential [3]. There are different device types such as inertial electrostatic confinement (IEC), plasma focus (PF), stellarator and magnetic toroidal chamber (TOKAMAK). They can be in spherical, cylindrical or toroidal shape in order to sustain the plasma for maximum confinement opportunities [2]. Another important point for the confinement is the potential distribution inside the effective plasma volume,

*Sorumlu Yazar (Corresponding Author)
e-posta : nmakgul@gmail.com

since the potential distribution governs the movement of ions in the vessel [4]. The charged particles (i.e. electrons and ions) can be directed to the central locations of the vessel for the best confinement activity, thereby maximum fusion reaction capability occurs [5]. In most of the experiments, the devices are first evacuated and filled with Deuterium via an ion gun till the pressure of about 0.1-10 mbar.

The leading concern about a new constructed plasma device is to understand the operation condition and provide the safety in terms of electrical, magnetic and radiation manner. Because plasma devices can generate a wide range of radiation starting from microwave to the gamma rays. Since the ionizing radiation has the leading importance, x rays, gamma rays and hard UV rays can be measured by nuclear counters. However, non-ionizing radiation is also vital for the health during the operation. Therefore, one should ascertain the limits of generated non-ionized radiation by measuring the surrounding of the device. For the non-ionizing radiation measurements, electromagnetic interference techniques (EMI) can be used.

EMI is electromagnetic energy emitted from sources that may cause undesirable situations in the operation of systems. All electrically powered devices, antennas and radars are potential sources of EMI around us. Electromagnetic compatibility is the ability of electrical or electronic devices to work in harmony with their environment in their electromagnetic environment. Electromagnetic compatibility standards are the basic structures developed for the determination of whether the systems can meet the performance requirements in the electromagnetic environments where they will operate [6].

Shielding is one of the most basic methods used to prevent electromagnetic interference. The main purpose of shielding is to keep the electromagnetic field within the boundaries of a certain region or to prevent it from entering a certain region [7,8].

Conductive materials are generally used as shielding material. The electromagnetic wave on the screen weakens in 3 stages. First, some of the incoming wave is reflected back from the screen surface. Secondly, some of the wave transmitted into the screen is absorbed by the screen. Thirdly, the electromagnetic wave undergoes multiple reflections on the screen [9,10]. The material to be used for shielding has a certain shielding efficiency. Shielding effectiveness (SE) is the ratio, in decibels (dB)

of the electromagnetic field intensity between the interference source and the victim without the screen to the electromagnetic field intensity when the screen is present. The higher the SE value, the better the shielding [11-14].

In this work, we analyze the EMI and shielding features of a new designed and constructed plasma device for a safe operation procedure in terms of non-ionizing radiation. The fundamentals of EMI are given in the next section. Measurement methods and characteristics of the cages used are given in Section 3. The experimental results and main discussion are given in Section 4. Finally, the paper ends with the concluding remarks.

2. MATERIAL and METHOD

The components creating the shielding effect are shown in Fig. 1. Electromagnetic waves are attenuated in three ways in a lossy wall: The first is reflections from the wall.

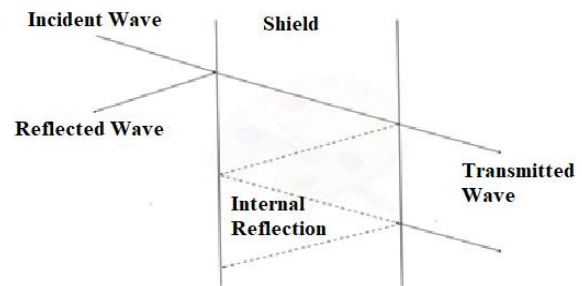


Figure 1. Attenuation of an electromagnetic wave by shielding technique.

The second is attenuation due to wall absorption. The third is the continuous reflection loss inside the wall. Shielding performance depends on the properties of the material. SE can be expressed as the sum of three contributions [15]:

$$SE = SER + SEA + SEMR \quad (1)$$

Here reflection and absorption losses and the multiple reflection are given by SER, SEA and SEMR, respectively. Within the frame of present work, the electromagnetic field measurements are obtained by using a Wavecontrol SMP2 device.

The SMP2 is a device with a range of compatible probes from 0 Hz to 40 GHz, used to measure electromagnetic fields. The SMP2 was developed to meet the needs of personal safety assessments in connection with exposure to electromagnetic fields and can be used in many different sectors and industries. In this work, WPF40 probe is chosen because the EM field range is within 20 MHz-40 GHz limits, electric field (E) and magnetic field (H) is selected as the area. Table 1 gives the conductivity (S/m) and permeability (H/m) values of some materials.

Table 1. Conductivity and permeability of some materials

Material	Relative conductivity, σ_r
Silver	0,1
Copper-annealed	1.00
Gold	0.7
Chromium	0.664
Aluminum (soft)	0.61
Aluminum (tempered)	0.4
Zinc	0.32
Beryllium	0.28
Brass	0.26
Cadmium	0.23
Bikel	0.20
Bronze	0.18
Platinum	0.18
Magnesium alloy	0.17
Tin	0.15
Steel (SAE 1045)	0.10
Lead	0.08
Monel	0.04
Conetic (1 kHz)	0.03
Mumetal (1 kHz)	0.03
Stainless steel (Type 304)	0.02

2.1. Measurement Method

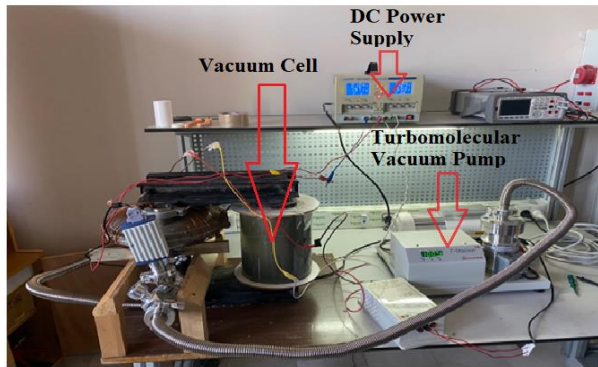
Determining the attenuation level of an EMI shield can be complex and research methods often vary with the particular shield application [16]. In addition to material properties such as conductivity and permeability, many factors such as frequency, place of measurement, polarization and incidence angle of the striking wave, near field or far field application affect EMI SE. There are many techniques to measure the EMI SE value [17]: The prominent ones are; first, coaxial transmission line method, second, shielded box method, third, rectangular waveguide method, etc. Fig. 2 presents a sample measurement.


Figure 2. A sample measurement screen of the measurement device.

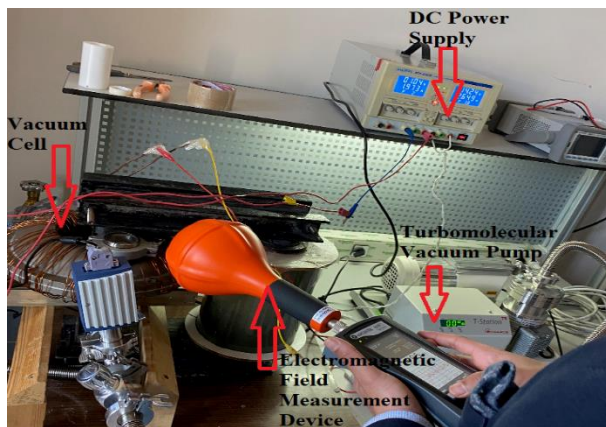
2.2. DC Plasma Device And Shielding Cages

The setup of the new constructed dc plasma device and its power sources and measurement equipment are shown in Fig. 3. The plasma device is at the left-hand side with stainless steel bright appearance having a torus shape. In the front of the device, an Inficon vacuum gauge exists for the pressure measurements. The poloidal and toroidal windings are also seen for the control of plasma inside the torus vessel. A low voltage dc power supply for the toroidal and poloidal windings exists at the top. Beside the long vacuum pump, dc high voltage source, which mainly drives the plasma is located. In addition, at the right-hand side a vacuum pump is situated for the pressure down and adjustment. Note that He gas tube exists just behind the plasma vessel and a second pump line contains the gas to the vessel via a vacuum valve. To conclude, the experimental unit basically includes a vacuum vessel, vacuum pump, low and high voltage power supplies.

The high voltage drive is provided by an electrode system positioned on the vessel wall. The potential difference inside the vessel forms the plasma in He media [18, 19]. Note that the insulators preserve the electrodes from any short circuit. The electrodes have two thick Wolfram square material and this configuration at the middle of the torus enables gas discharge and accelerates charged particles along a torus shape. Note that potential region for such a system depends on the gas pressure due to the Paschen law and from positive electrode to the negative one. This decreasing potential enforces electrons to move from the cathode to anode as shown in Fig. 4. Note that CST Particle Studio package has been used under $p=1$ mbar and $U=-500$ V.



(a)



(b)

Figure 3. The setup for the measurement of the plasma device, (a) setup, (b) measurement

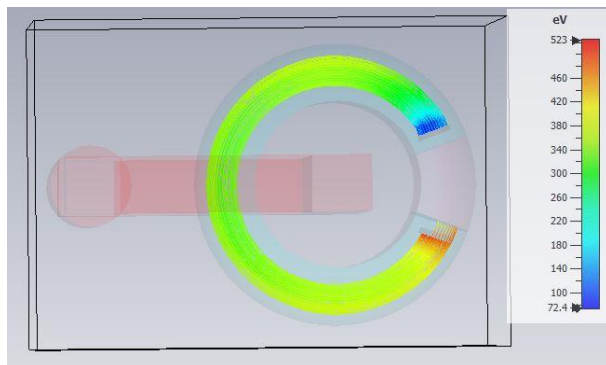


Figure 4. The simulation of electron trajectories due to the potential difference between the electrodes via the CST Particle Studio at $p=1$ mbar; $U=-500$ V.

According to our methodology, three cages with different features are used for the EM shielding studies. Initially, the plasma device is operated with without any cage in order to define the radiation generated by the plasma device. Before the system operate, we calibrate the background radiation in the laboratory. Then, the measurements are taken at different distances from the device and recorded in a systematic way. At this stage, the measurements are performed with 3 cages whose dimensions are 60x60x40 cm, under the names of swatter, honeycomb and square from front, side and top faces of the system. The swatter material used as shielding is wire mesh with a diameter of 0.1 cm and consists of stainless steel and it is shown in Fig 5.The

honeycomb material used as shielding is wire mesh with a diameter of 1 cm and consists of steel and it is shown in Fig 6. The square material is wire mesh with a diameter of 0.5 cm and consists of steel and it is shown in Fig 7.



Figure 5. Shielding material of swatter type.

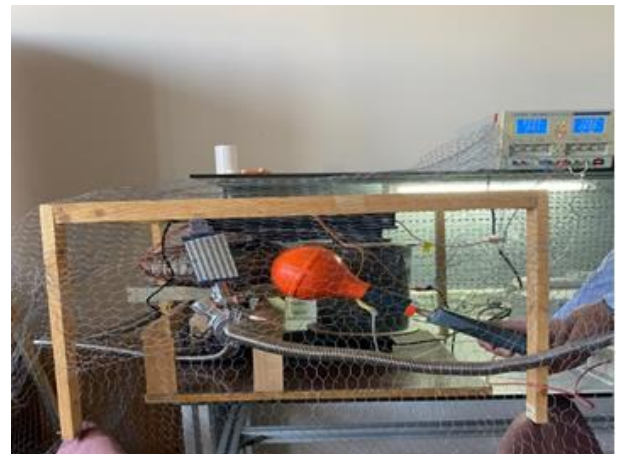


Figure 6. Shielding material of honeycomb type.

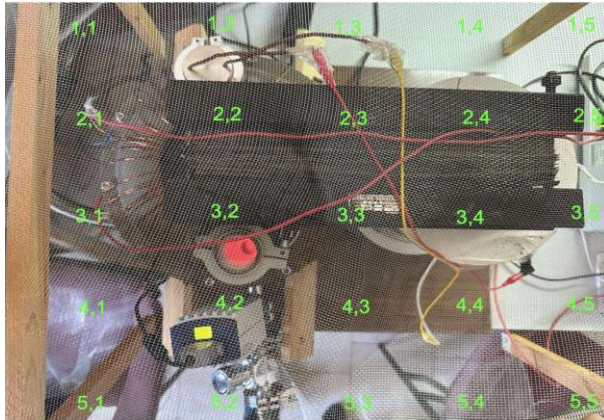


Figure 7. Shielding material of square type.

4. EXPERIMENTAL RESULTS AND DISCUSSION

At least 25 measurements from three directions of the rectangular shielding box are made by using three types of metal cages (i.e, square, swatter, honeycomb). For this, 10 cm intervals are adjusted to get data for each surface for the complete radiation effect. Note that the measurement probe has been used from different sides of the cage (i.e. front, side, top). The positional

representation of 25 measuring points for plasma is shown in Fig. 8 for the swatter type cover.



(a)



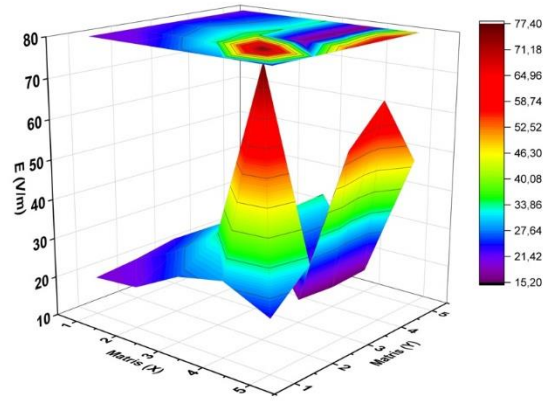
(b)



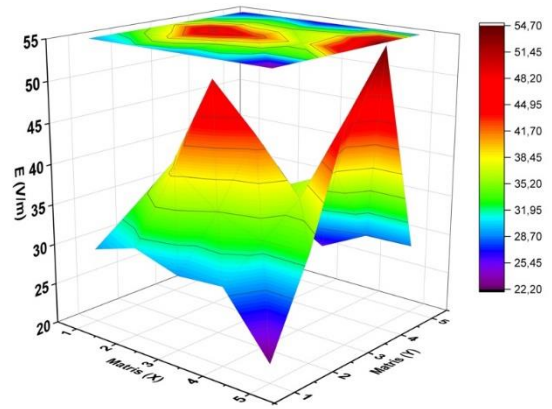
(c)

Figure 8. Positional representation of 25 measuring points for plasma from (a) top, (b) side, and (c) front

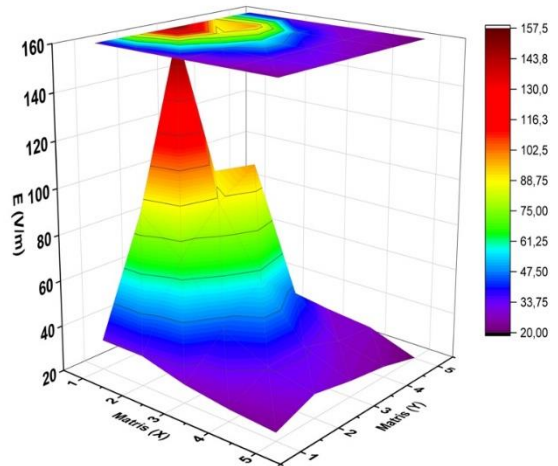
Between Figs. 9(a,b,c) and Figs. 12(a,b,c), the 3D plots of electric field with surface drawings are presented from the sides namely, front, side and top. According to the tests, when the distance from the cage is increased, it has been proven that the EM values (i.e. E and H) for all regions decrease as usual (Figs. 9(a,b,c)).



(a)



(b)



(c)

Figure 9. Electric field measurements from (a) front, (b) side, and (c) top without any shielding, when the plasma system operates.

Without any shielding, when the plasma device operates, the electric field values in Fig. 9(a,b,c) are measured from the front, side and top. The highest field values are

obtained at top with $E = 157.5 \text{ V/m}$ at the coordinate (x,y) $(1,3)$ at top, whereas, the minimum field is obtained at front with $E = 15.92 \text{ V/m}$ at the coordinate $(4,5)$. The maximum field value coincides with the torus shaped plasma device, then the values gradually decrease till the location of the toroidal current windings. Especially Figs. 9(a,b) prove that the leakage flux emitted from the core of the electromagnet causes 25 V/m radiation at the front of the system. From the side view, the horizontal component of the field gives 23 V/m at the location of windings. Around the vessel, lower value is obtained. The reason is that the stainless steel vessel shields some of the emitted radiation. Therefore, from the top vies, around 38 V/m field value is observed at the location of vessel, whereas it reaches to 67 V/m at the vicinity of core and windings. Note also that the core part of the machine is much closer to the top compared to the vessel, thereby it is reasonable to have relatively low value of radiation.

Figs. 10(a,b,c) present the overall electromagnetic characteristics of the plasma with honeycomb type shielding material. The highest electromagnetic values are obtained for the honeycomb at top with 33.6 V/m at the coordinate $(1,3)$, whereas, the minimum is obtained at front with 3.2 V/m at the coordinate $(4,4)$. Note that the maximum values coincide with the core, windings and vessel as in Fig. 9(a,b,c). It is also obvious that the highest value in Fig. 9(c) decreased to half of the shielding-free case, when compared with the results in Fig. 10(c).

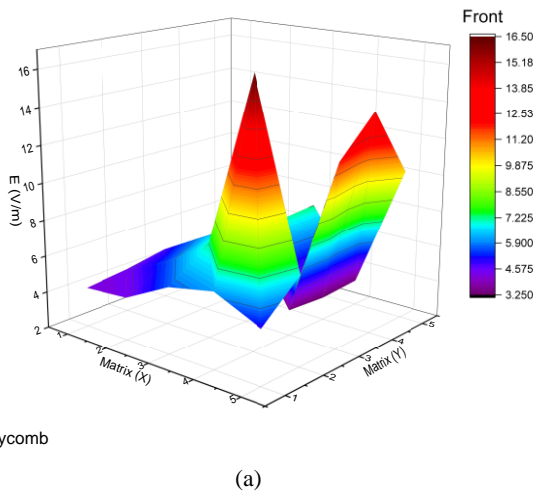
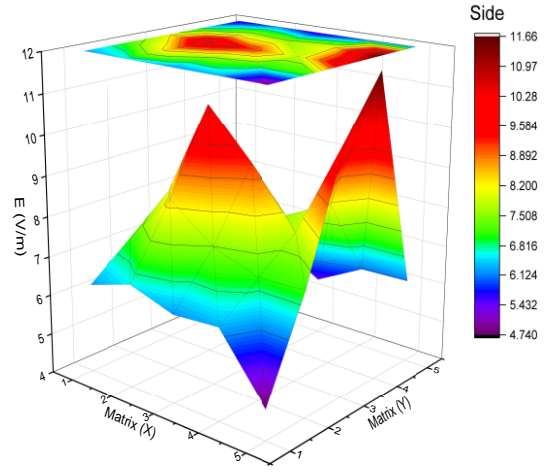
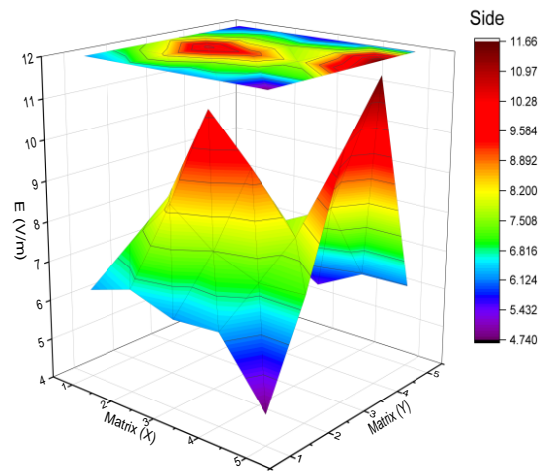


Figure 10. Electric field measurements from (a) front, (b) side, and (c) top with honeycomb shielding, when the plasma system operates.



Honeycomb

(b)

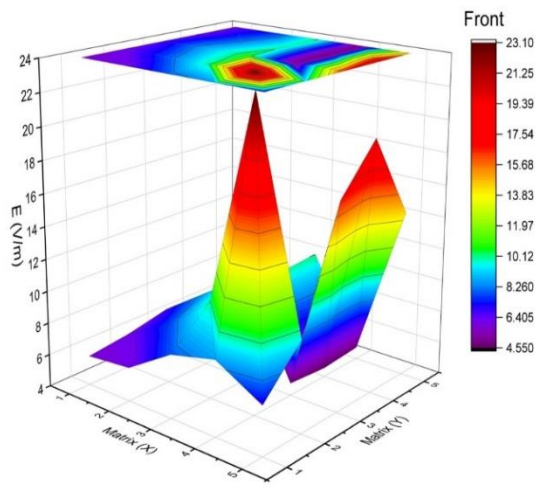


Honeycomb

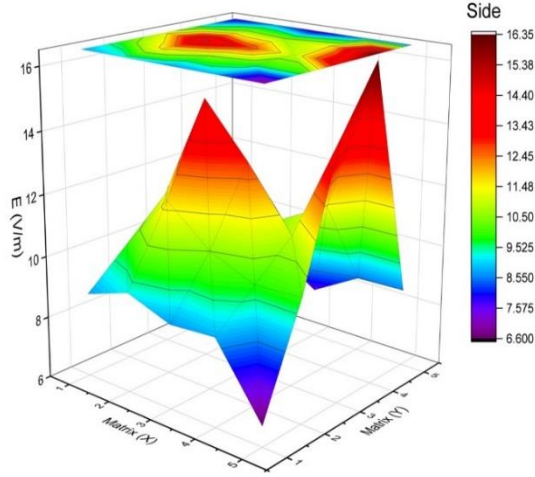
(c)

Figure 10 continue. Electric field measurements from (a) front, (b) side, and (c) top with honeycomb shielding, when the plasma system operates.

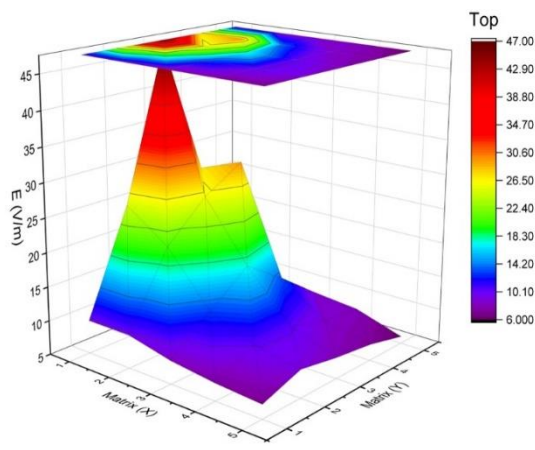
Figs. 11(a,b,c) give the overall electromagnetic characteristics of the plasma with square shielding material. The highest electromagnetic values are obtained for the square at top with $E = 47 \text{ V/m}$ at the coordinate $(1,3)$, whereas, the minimum is obtained at the front with $E = 4.55 \text{ V/m}$ at the coordinate $(4,4)$. The maximum field locations coincide with the vessel, core and windings as in other measurements.



Square
(a)



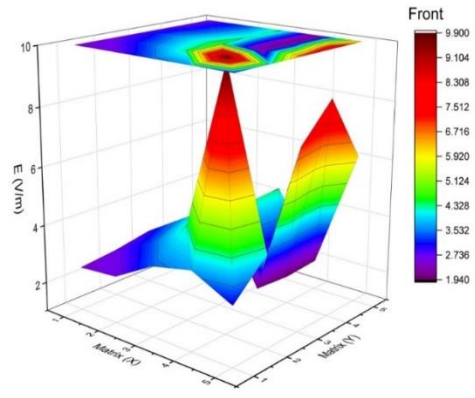
Square
(b)



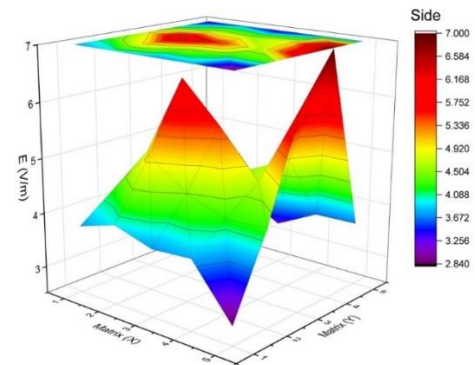
Square
(c)

Figure 11. Electric field measurements from (a) front, (b) side, and (c) top with square shielding, when the plasma system operates.

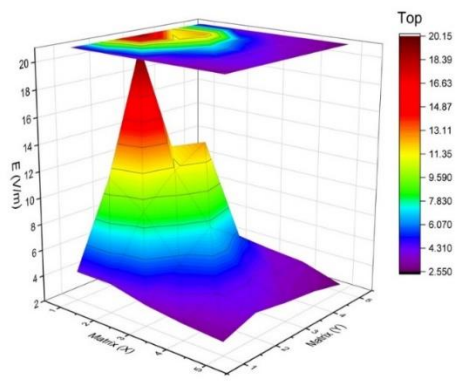
Figs. 12(a,b,c) present the overall electromagnetic characteristics of the plasma system with a swatter type shielding material. From the front of the system, maximum and minimum fields are found to be 9.9 V/m at the coordinate (4,2), 1.94 V/m at the coordinate (4,4), respectively as shown in Fig. 12(a). The highest field emission is obtained for the swatter at top with $E = 20.15$ V/m at the coordinate (1,3), whereas, the minimum is obtained at front with $E = 1.94$ V/m at the coordinate (4,4).



Swatter
(a)



Swatter
(b)



Swatter
(c)

Figure 12. Electric field measurements from (a) front, (b) side, and (c) top with swatter shielding, when the plasma system operates

It is obvious from Figs. 12(a,b,c) that the field value is the highest for top, moderate for the side and lowest for front measurements. Considering all measurements, when the shielding is applied to the system, a substantial decrease in the field is observed. At least 1/3 of shielding-free value can be obtained in that manner when the shielding is practiced. These values prove that a significant decrease in electric field values are shown for the swatter cage compared to the honeycomb and square cages.

Fig. 13, gives the overall electromagnetic characteristics of the plasma with swatter cage and without the cage for 0-30 cm distance from the shielding cage. The swatter is used in this comparison graph because the best shielding value has been measured for the swatter type material.

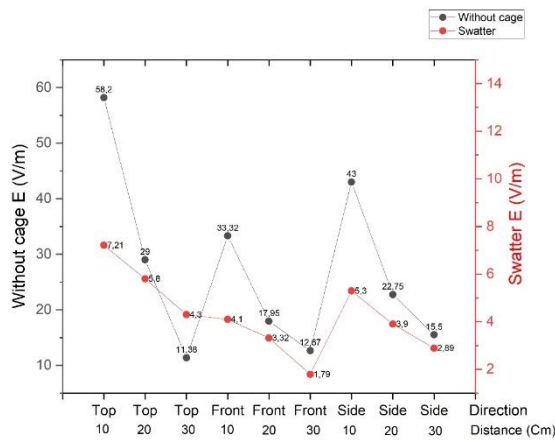


Figure 13. Electric fields versus the distance in cm from the shielding cage for the swatter (red) and shielding-free cases (black).

In both cases, it is clearly observed that the electric field value decreases by the distance as usual. The highest fields are measured at top with 10 cm distance, whereas the lowest fields are found at front for 30 cm. This comparison also proves the positive effect of the shielding to prevent the surroundings from the non-ionizing radiation.

In order to identify the shielding effect, we have also searched the inner part of shielding cover. For this purpose Fig. 14 has been plotted from our experiments.

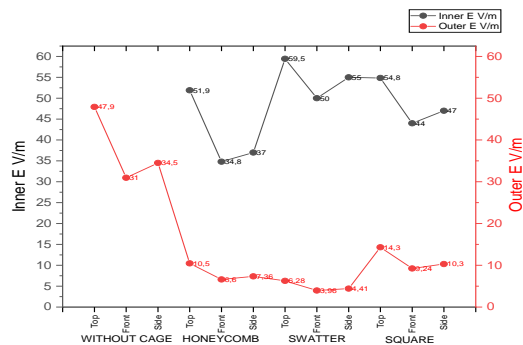


Figure 14. Inner/Outer electromagnetic field

Note that the outer electromagnetic field recorded from the averaged values of the measurements for the validation. In the case of shielding-free, the highest values of outer electromagnetic fields are found as $E = 47.9$ V/m in average at top. After applying the shielding, the field is decreased linearly on the outside and reached the lowest average value of $E = 3.96$ V/m for the swatter at front. In contrast to the outer electromagnetic field, the field shows the similar trends for each shielding method. Besides, the highest field value is measured at top and the lowest one in the front. As seen in Fig. 14, the highest inner electromagnetic field is top in the swatter cage as a 59.5 V/m.

Fig. 15 summarizes the SE value at three directions for three shielding materials. The highest shielding value is provided by the swatter at different directions. A shielding value of over 20 dB is only provided for the swatter. On the contrary, maximum values of 14.4 dB and 13.6 dB are obtained for the honeycomb and square materials, respectively.

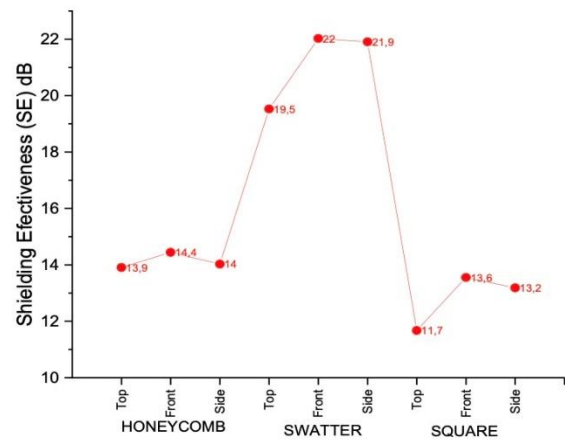


Figure 15. The shielding effectiveness of the plasma device for different shielding methods.

Considering all materials used, the swatter geometry is appropriate due to the wavelength of the generated field, thereby compared to the other shielding types, it is found to be more successful. This should be also noted that the generated radiation wavelength may change from one device to other. Therefore, for different devices, one should work on which is the most suitable shielding type. The main motivation of this work explains this idea clearly. Besides, the conductivity of the shielding material is also important. The increase in conductivity parameter improves the capability of SE, however the most important point here is the wavelength fit of the shielding material. In this manner, the successive distance on the swatter conducting materials on the surface is lower than that of honeycomb and square geometries. This point is the most important reason to be the best shielding material in this application.

In conclusion, a material with an attenuation level between 90 dB and 120 dB is considered to have

excellent shielding performance. Any calculated attenuation greater than 100 dB means that the material is essentially impenetrable according to Ref. [18, 19]. SE values lower than 10 dB gives weak shielding effect, whereas 10dB-30 dB can be acceptable for shielding and the value 30 dB exceeds the acceptable value of 20 dB for all industrial and commercial applications as reported in Ref. [14]. In our case, the shielding worked her having a shielding effectiveness above with 20 dB for swatter, thereby, it provides a significant degree of attenuation of the electromagnetic non-ionizing radiation.

4. CONCLUSION

The electromagnetic interference (EMI) measurements of a new designed and constructed DC discharge plasma device is performed. As the methodology, different shielding materials with different geometries are applied. The tests prove that the best shielding effectiveness for the new plasma device from all of the directions is provided by the swatter cage material since it gives the best fit for the wavelength of the generated radiation. Strictly speaking, it has been concluded that the SE value of the swatter protection is over 20 dB and has better performance than the honeycomb and square shieldings. During the work, the most powerful field is measured on top due to the location of cores of the feeding toroidal electric field windings. In addition, the vessel with the discharge phenome inside also show high radiation emission. Since the working voltage of He gas plasma is between $U = 500$ V and $U = 2$ kV depending on the filled gas pressure in the vessel, the generated radiation wavelength may change, however, we expect mostly swatter type shielding material can prevent the surroundings from the non-ionizing radiation. As the second conclusion, the field values decrease by distance from the cages, and good shielding effects have been noted compared to the without cage cases following the detailed measurements.

ACKNOWLEDGEMENT

For the interest and support, We thank Gazi University.

DECLARATION OF ETHICAL STANDARDS

The authors of this article declare that the materials and methods used in this study do not require ethical committee permission and/or legal-special permission.

AUTHORS' CONTRIBUTIONS

Nihan Merve SARIKAHYA: Performed the experiments and analyse the results. Wrote the manuscript.

Mehmet SARIKAHYA: Performed the experiments and analyse the results. Wrote the manuscript.

Erol KURT: Performed the experiments and analyse the results. Wrote the manuscript.

CONFLICT OF INTEREST

There is no conflict of interest in this study.

REFERENCES

- [1] Kurt, E., Arslan, S., Güven, M.E., "Effects of Grid Structures and Dielectric Materials of the Holder in an Inertial Electrostatic Confinement (IEC) Fusion Device". *J. Fusion Energy*, 30: 404–412, (2011).
- [2] Xu, Y., "A general comparison between tokamak and stellarator plasmas", *Matter and Radiation at Extremes*, 1:192-200, (2016).
- [3] Dursun, B., Kurt, E., "Electromagnetic Design and Simulation of a New Fusion Device", *Elektronika ir Elektrotechnika*, 20(8):34-38, (2014).
- [4] Dursun, B., Kurt, E., Tekerek, M., "A power circuit design for the poloidal field coils in a torus shaped plasma system", *J. Energy Systems*, 3:3, (2019).
- [5] Kurt, E., "A stationary multi-component cathode modeling and ion trajectories for an inertial electrostatic confinement fusion device", *Int. J. Energy Research*, 35:89 – 95,(2011).
- [6] Robinson, M.P., Benson T.M, Christopoulos C., Dawson J.F., Ganley M.D., Marvin A.C., Porter S.J., Thomas D.W.P., "Analytical formulation for the shielding effectiveness of enclosures with apertures", *IEEE Transactions on Electromagnetic Compatibility*, 40(3):240-248, (1998).
- [7] Celozzi, S., Araneo, R., Lovat, G., "Electromagnetic Shielding, in Wiley Encyclopedia of Electrical and Electronics Engineering", Wiley, 1:42 ,(2008).
- [8] Caramitu, A.R., Ioana, I. & Bors, A. M., Tsakiris, V., Pintea, J., Caramitu A.D. "Preparation and Spectroscopic Characterization of Some Hybrid Composites with Electromagnetic Shielding Properties Exposed to Different Degradation Factors", *Materiale Plastice*, 59: 82-94, (2023).
- [9] Merizgui, T., Abdechafik, H, Mecheri, K., "Modelling and Measurement of Electromagnetic Shielding Effectiveness", 2018 International Conference on Electrical Sciences and Technologies in Maghreb (CISTEM), Algeria:1-6, (2018).
- [10] Tunakova, V, Militky, J. "Multifunctional metal composite textile shields against electromagnetic radiation—effect of various parameters on electromagnetic shielding effectiveness". *Polymer Composites*, 38 :309–323, (2017).
- [11] Wanasinghe, D., Aslani, F., Ma, G., "Electromagnetic shielding properties of carbon fibre reinforced cementitious composites", *Construction and Building Materials*, 260:19-27, (2020).
- [12] Wang, Y., Wanga, W., Dinga, X., "Multilayer-structured Ni-Co-Fe-P/polyaniline/polyimide composite fabric for robust electromagnetic shielding with low reflection characteristic", *Chemical Engineering Journal* , 380: 91-103, (2020).
- [13] Wypych, G., "Handbook of Fillers", 28, Pigment & Resin Technology, United Kingdom, (1999).

- [14] Afilipoaei, C., Teodorescu-Draghicescu, H., “A Review over Electromagnetic Shielding Effectiveness of Composite Materials”, *Proceedings*, 63: 23; (2020).
- [15] Safarova, V., Militky, J., “Multifunctional Metal Composite Textile Shields Against Electromagnetic Radiation—Effect of Various Parameters on Electromagnetic Shielding Effectiveness”, *Society of Plastics Engineers.*, 38:309–323, (2017).
- [16] Mathur, P., RAMAN, S., “Electromagnetic Interference (EMI): Measurement and Reduction Techniques”, *Journal of Electronic Materials*, 49: 5-18, (2020).
- [17] Munalli, D., Dimitrakis, G., D. Chronopoulos, “Electromagnetic shielding effectiveness of carbon fibre reinforced composites”, *Composites* , (2019).
- [18] Kurt, E, Kurt, H., Bayhan, U., “Ionization Effects and Linear Stability in a Coaxial Plasma Device”. *Cent. Eur. J. Phys.* 7: 123–129, (2009).
- [19] Kurt, E., Arslan, S., “An Inertial Electrostatic Confinement (IEC) Device Modeling and the Effects of Different Cathode Structures to the Fields”, *Energy Conversion and Management*, 63: 55-62, (2012)